MATERIALS AND METHODS

Fluorescent polystyrene nanospheres

Yellow-green fluorescent carboxylated polystyrene nanospheres of nominal size 0.1 µm and 0.2 µm were purchased from Invitrogen (Merelbeke, Belgium). To avoid adsorption of the nanospheres to the microscope slides, the nanospheres were coated with Pluronic F-127, a block-copolymer of polyethyleneglycol (PEG) and polypropylene oxide, which was purchased from Sigma Aldrich (Bornem, Belgium). The coating procedure was carried out as previously described[1]. In short, 150 µl of the nanosphere stock suspension was sonicated for 10 minutes and mixed with 850 µl distilled water as well as 2 ml of a Pluronic F-127 solution in distilled water. After vortexing and a 1h incubation period at room temperature, the nanosphere suspension was transferred to centrifugal filter devices (MWCO 100,000; Microcon YM-100; Millipore, Bedford, MA) and centrifuged for 12 min at 14,000g. The sample reservoirs were subsequently placed upside down in new vials and centrifuged for 3 min at 1000g to collect the coated nanosphere concentrates. Finally, the coated nanospheres were resuspended by adding 200 µl of HEPES buffer (20 mM HEPES, pH 7.4).

Liposomes

Cationic liposomes were made out of equimolar amounts of the cationic lipid 1,2-dioleyl-3-trimethylammoniumpropane (DOTAP) and the neutral fusogenic lipid 1,2-dioleoyl-*sn*-glycero-3-phosphoethanolamine (DOPE). The liposomes were fluorescently labeled by incorporation of 0.1 mol% DOPE-LissamineRhodamineB (λ_{ex} = 557 nm, λ_{em} = 571 nm). All lipids were purchased from Avanti Polar Lipids (Alabaster, AL). Functionalisation of the DOTAP-DOPE liposomes with polyethylene-glycol (PEG) chains was done through the addition (3, 5 and 10 mol%) of 1,2-distearoyl-*sn*-glycero-3-phosphoethanolamine-N-[methoxy(polyethylene glycol)-2000] (DSPE-PEG) or N-palmitoyl-sphingosine-1-{succinyl[methoxy(polyethylene glycol)2000]} (C16 PEG-Ceramide). To prepare the liposomes, the lipids were dissolved in chloroform and mixed in a round bottomed flask. A lipid film was formed by rotary evaporation of the chloroform at 40 °C. The dried lipid film was rehydrated with 20 mM Hepes buffer pH 7.4, resulting in a final concentration of 5 mM DOTAP, 5 mM DOPE and a suitable concentration of DSPE-PEG or C16 PEG-Ceramide. The lipid film was allowed to hydrate resulting in liposome formation. Finally, the liposomes were extruded 11 times (at room temperature) through a polycarbonate membrane filter with 100 nm pores (Whatman, Brentfort, UK).

Cell-derived microparticles

Cell-derived MPs were released from endothelial cells (HMEC, human microvascular endothelial cells) in culture upon stimulation with TNFα (100 ng/ml for 24 h) as previously described[2]. The endothelial-derived MPs were isolated from the supernatant of stimulated cultures by sequential centrifugation, first at 1500g for 15 min followed by 15000g for 2 min to eliminate cells and cell debris. MPs in the cleared supernatant were sedimented at 20000g for 90 min, washed with 2 ml of

HEPES (0.15 M NaCl, 10 mM HEPES, pH 7.4) buffer and then resuspended in 100 µL of the same buffer. This was repeated two times. Before testing, the isolated MPs were resuspended in microparticle-free undiluted plasma and were incubated with one of the following fluorescently labelled probes: annexin V or antibodies directed against uPA (urokinase-type plasminogen activator), CD105 (endothelial cluster of differentiation membrane molecule) or the platelet cluster of differentiation molecule CD41 (negative control).

Collection of human blood samples

Whole blood was freshly collected from healthy volunteers in Li-heparine tubes (Terumo Europe, Leuven, Belgium). For the preparation of plasma, the blood tubes were centrifuged for 30 minutes at 700g in a swinging bucket centrifuge (Heraeus Multifuge 1 S-R, DJB Labcare, Newport Pagnell, UK). Human serum was collected in Venoject tubes containing a clotting activator and a separation gel (Terumo Europe, Leuven, Belgium). The blood was allowed to clot for 30 minutes before 30 minutes centrifugation at 700g. All sizing experiments were carried out on the same day at which the blood samples were collected.

Fluorescence SPT sizing in whole human blood

For nanoparticles sizing in whole blood, plasma or serum, a simple artificial blood circulation system was set up (see Fig. S5) consisting of tubing with 1.6 mm inner diameter (Helix medical, Carpinteria, CA, USA) and a peristaltic pump (BL 760 FB, Bellco, Mirandola, Italy). The tubing inner diameter and the speed of the peristaltic pump were selected as to obtain a fluid velocity of approximately 5 ml/min, which corresponds to the situation in the lateral tail veins of rats. The entire blood circulation system was incubated at 37°C. The liposome stock dispersions were first diluted 1/50 in Phosphate Buffered Saline (PBS) and a volume of 200 µl was injected into 5 ml of blood in the circulation system. At regular time intervals after injection, a 5 µl sample was taken from the blood circulation and transferred to a microscope slide (as described further on), which was put on the microscope stage and allowed to reach a temperature of 37°C before starting the SPT measurements.

Viscosity measurements

The dynamic viscosity η of human serum and plasma samples was determined by measuring their density ρ and kinematic viscosity ν and making use of the relation $\eta = \rho \times \nu$. The kinematic viscosity was measured with a capillary viscosimeter (model PVS1; Lauda, Lauda-Königshofen, Germany). The density was determined with a picnometer. The dynamic viscosity of both human plasma and human serum was found to be constant at approximately 1.35 cP over 24h (measured at 37°C) and varied less than 0.02 cP between different donors. For all SPT measurements a value of 1.35 cP was used.

***In vivo* experiments**

8-weak old male Sprague-Dawley rats (Elevage Janvier, Le Genest Saint Isle, France) were injected in the lateral tail vein with 200 µl of the appropriate liposome dispersion diluted in sterile PBS. At regular time intervals, a blood sample (approximately 50 to 100 µl) was collected in Li-Heparin containing Microvette tubes (Sarstedt, Nümbrecht, Germany) through lateral tail vein puncture in the vein opposite to the one used for injection. The animals were housed and handled according to the regulations of the Belgian Government. All animal studies were approved by the Ghent University local ethical committee.

DLS measurements

Dynamic light scattering (DLS) measurements were carried out on a Nano-ZS (Malvern; Worcestershire, UK). The zeta potential was also measured by determining the electrophoretic mobility (in 20 mM Hepes buffer pH 7.4) on the same instrument. The zeta potential ζ of the liposomes was typically around + 50 mV for the non-pegylated liposomes, and around + 15 mV for the pegylated liposomes.

Fluorescence SPT set-up

The SPT experiments were carried out on a custom-built laser widefield epi-fluorescence microscope set-up. Three solid state lasers are used for illumination: a 100 mW Calypso 491 nm (Cobolt, Solna, Sweden), a 75 mW Jive 561 nm (Cobolt) and a IQ1C 30 mW 636 nm (Power Technology, Little Rock, AR). The laser beams pass through an acousto-optic tunable filter (AOTF; AA Optoelectronic, Orsay, France) which allows to control the intensity of the individual laser lines independently. The AOTF is synchronized to the CCD camera in order to illuminate the sample only during the light integrating phase and thus to reduce photobleaching. The collimated laser beams are directed through a 5° Light Shaping Diffuser (Physical Optics Corporation, Torrance, CA), which in combination with an achromat lens in front of the microscope entrance provides widefield Kohler illumination at the sample. The microscope is a Nikon TE2000E (NIKON BELUX, Brussels, Belgium) with a Nikon Plan Apochromat 100× NA1.4 oil immersion objective lens. An objective inverter (LSM Technologies, Etters, PA) is used so that the objective lens is situated above the microscope sample. This is useful when observing blood samples in which the erythrocytes will sediment to the bottom of the microscope slide leaving the particles diffusing in the plasma on top of that, closest to the lens. The fluorescence light coming from the sample is collected again by the objective lens and sent through the side port of the microscope towards the CCD camera. The fluorescence light is separated from the laser excitation light using a custom triple chroic mirror and accompanying laser notch filter obtained from AHF Analysentechnik (Tübingen, Germany). A pair of achromat lenses was placed in between the CCD camera and microscope side exit for an extra 2× magnification of the final image on the CCD chip such that one pixel corresponds to a distance of 89 nm in the sample. Since fast and sensitive image capture is required for SPT, an electron multiplying CCD camera was used (Cascade II:512; Roper Scientific, Tucson, AZ). The image acquisition was done using the Nikon Elements R imaging software.

Fluorescence SPT experimental protocol

Our custom-built single particle tracking setup uses widefield laser illumination to efficiently excite the fluorescently labeled particles, as described above. High-speed movies are recorded of individual particles diffusing in the suspension. Using custom developed software the movies are analyzed to obtain the motion trajectories of all individual particles. By calculating the diffusion coefficient for each trajectory, a distribution of diffusion coefficients can be obtained which can be transformed to a size distribution with the Stokes-Einstein equation. The raw size measurement is finally refined by a Maximum Entropy deconvolution process which eliminates statistical broadening of the distribution and sampling noise (See 'Theory' in Supporting Information).

For SPT sizing, 3 to 5 µl of the sample (with typical concentration of 10^9 to 10^{12} particles per ml) was applied between a microscope slide and a cover glass with a double-sided adhesive sticker of 120 µm thickness in between (Secure-Seal Spacer; Molecular Probes, Leiden, The Netherlands). This provides for a 3-D environment in which the particles can diffuse freely, while the sample is sufficiently thin to avoid drift from convection[3].

All SPT experiments were carried out at 37°C by using an objective heater system (Bioptechs, Butler, PA) in combination with a warm stage (Linkam, Waterfield, United Kingdom) for heating of the sample. Each sample was allowed to equilibrate for 2 minutes on the microscope stage before starting the fSPT experiments.

To increase the image capture rate, a subregion of the CCD chip was selected of 256 rows by 512 columns. Typical illumination times were between 1 and 4 ms per frame, which yields a frame rate of approximately 40 to 45 frames per second. For each sample typically 10 to 20 movies of about 200 frames were recorded at different locations within the sample. The microscope was always focused between 5 and 10 µm from the cover glass to avoid deviations from free diffusion due to the presence of the cover slip [4]. During the measurements the focus position was held constant by the Nikon Perfect Focus System.

Fluorescence SPT image analysis

Analysis of the SPT movies was performed off-line. Custom image processing software was developed for tracking of the individual particles, which is explained in detail elsewhere [5]. In short, the particles are first identified in all frames of the SPT movie using an unsharp filter and automatic intensity thresholding. For each identified particle, the intensity weighted centre is calculated along with several other quantities, such as the apparent size, surface area, intensity etc. A nearest neighbor algorithm then calculates trajectories of individual particles.

Size calculations from fluorescence SPT data

As discussed in the theory section, the MEM analysis requires trajectories of a constant number of steps. Typically, a minimum trajectory length of 10 steps was selected. Trajectories with fewer steps were not included in the analysis, while for longer trajectories only the 10 first steps were effectively

used. Next, the mean square displacement $\bar{\xi} = \frac{1}{K}\sum_{i=1}^{K}\left|\vec{r}_i - \vec{r}_{i-1}\right|^2$ was calculated for each trajectory from which the empirical diffusion coefficient was derived according to $D_e = \bar{\xi}/4t$, where *t* is the time between the subsequent trajectory locations (i.e. the time between the subsequent frames in the SPT movie). It should be noted that 2-D diffusion analysis is valid here. This is because the particle locations can only be determined in 2-D (*x*- and *y*-coordinates, parallel to the focal plane) from the microscopy images, although the nanoparticles are diffusing in 3-D. However, this is not a problem since we are dealing with isotropic diffusion which allows to analyze the diffusion for each direction (*x*, *y* or *z*) independently. All empirical diffusion coefficients as derived from individual trajectories from particles belonging to the same sample were then pooled in order to create the corresponding empirical cumulative distribution function (ecdf). The MEM procedure analyzed the ecdf and returned the 'true' underlying distribution of diffusion coefficients. Finally, the distribution of diffusion coefficients was converted to a size distribution using the Stokes-Einstein relation for spherical particles (see Eq. 3 in 'Theory' of Supporting Information). The size distributions are visualized as the relative frequency α_i with which a size d_i is present in the particle population (also see the 'Theory' section in the Supporting Information). For each size distribution, the sum of all frequencies equals 1: $\sum \alpha_i = 1$. Throughout this manuscript, the ordinate axis of the size distributions is labeled as '*f*', which is the more conventional notation for 'frequency', rather than α.

Let it be noted that the size distributions as calculated from SPT reflect number distributions as opposed to DLS size distributions which are intensity weighted (larger particles scatter more light and thus contribute more to the final distribution). Future work of ours is aimed at converting the number of trajectories that are observed to absolute particle number concentrations. This is not a trivial matter because of the inherent sampling bias that is present for polydisperse particle distributions: small particles move more rapidly through the focal plane and will give rise to a higher number of trajectories as compared to a similar concentration of larger particles. Similarly, a compensation needs to be introduced for setting a lower threshold on the minimum number of steps for the trajectories that are analyzed by MEM. Alternatively, we are working on an improved analysis model that does not require the rejection of shorter trajectories. This work will further extend the usefulness and applicability of the fSPT sizing method to e.g. quantitative extravasation studies.

THEORY

In this section we will discuss in detail the theory of sizing particles by fSPT and the maximum entropy analysis. First consider a particle diffusing with diffusion coefficient *D* in a solution. With the fSPT technique a movie is recorded in which the movement is sampled, resulting in a 2-D diffusion trajectory of *K*+1 locations $\vec{r}_0,\vec{r}_1,\ldots,\vec{r}_K$ (i.e. *K* steps). The mean square displacement $\bar{\xi}=\frac{1}{K}\sum_{i=1}^{K}\left|\vec{r}_i-\vec{r}_{i-1}\right|^2$ follows the distribution [6]:

$$f\left(\bar{\xi}\right)\mathrm{d}\bar{\xi}=\frac{K^K\bar{\xi}^{K-1}}{(K-1)!}\frac{1}{(4Dt)^K}e^{-K\bar{\xi}/4Dt}\mathrm{d}\bar{\xi}\,. \tag{1}$$

Since $\bar{\xi}=4D_et$, where D_e is the *empirical* diffusion coefficient as calculated from the trajectory, the distribution of D_e is given by:

$$f\left(D_e\right)\mathrm{d}D_e=\frac{K^K{D_e}^{K-1}}{(K-1)!D^K}e^{-KD_e/D}\mathrm{d}D_e=f_\gamma\left(D_e;K,\frac{D}{K}\right)\mathrm{d}D_e\,, \tag{2}$$

where f_γ denotes the gamma density function. The corresponding expectation value is $\mu=E\left(D_e\right)=D$ and the variance is $\sigma^2=D^2/K$. Thus we find for the coefficient of variation $\sigma/\mu=K^{-1/2}$, from which it is noticed that the precision with which the diffusion coefficient can be calculated from a single trajectory increases with an increasing number of steps *K* in that trajectory.

Now consider a population of particles dispersed in a solution and having a polydisperse size distribution. According to the Stokes-Einstein relation, each particle will be characterized by a diffusion coefficient

$$D=\frac{kT}{3\pi\eta d} \tag{3}$$

where *k* is the Boltzmann constant, *T* the absolute temperature, η the dynamic viscosity of the solution, and *D* the diffusion coefficient of the particle. If $\alpha\left(D\right)$ represents the real distribution of diffusion coefficients of the population of particles, then the distribution of the empirical diffusion coefficients becomes:

$$f\left(D_e\right)\mathrm{d}D_e=\int\alpha\left(D\right)f_\gamma\left(D_e;K,\frac{D}{K}\right)\mathrm{d}D\,\mathrm{d}D_e \tag{4}$$

$f\left(D_e\right)$ thus represents the distribution of empirical diffusion coefficients as would be obtained from fSPT trajectories consisting of *K* steps. In order to obtain the real distribution of diffusion coefficients $\alpha\left(D\right)$, we will make use of a Maximum Entropy deconvolution method. To this end, the

(continuous) distribution $\alpha(D)$ is approximated by a discontinuous system consisting of *N* fractions α_i with diffusion coefficients D_i. Eq. (4) then becomes:

$$f(D_e)\mathrm{d}D_e = \sum_{i=1}^{N} \alpha_i f_\gamma\left(D_e; K, \frac{D_i}{K}\right)\mathrm{d}D_e, \tag{5}$$

where $\sum_{i=1}^{N} \alpha_i = 1$ and $\alpha_i \geq 0$. Let it be noted that Eq. (5) assumes an identical trajectory length of *K* steps for all particles. For the corresponding cumulative distribution we find:

$$F(D_e) = \int_0^{D_e} f(D_e)\mathrm{d}D_e = \sum_{i=1}^{N} \alpha_i \frac{\gamma(K, D_e K/D_i)}{\Gamma(K)} \tag{6}$$

where $\gamma(a,x) = \int_0^x t^{a-1}e^{-t}\mathrm{d}t$ is the incomplete gamma function and $\Gamma(K) = (K-1)!$ since *K* is a positive integer. By calculating the empirical cumulative distribution function (ecdf) of empirical diffusion coefficients, the underlying distribution of diffusion coefficients coefficients $[D_1,\ldots,D_N]$ with fractions $[\alpha_1,\ldots,\alpha_N]$ can be obtained using Eq. (6). However, rather than performing a standard least squares fit of Eq. (6) to the ecdf, we will analyze the ecdf by the 'maximum-entropy' method which finds the 'best-fit' solution that has maximum entropy[7,8]. The maximum-entropy method (MEM) ensures that the best-fit solution is found that has the least information in order to avoid over-interpretation of noise (due to limited sampling statistics). In this work we have implemented the 'historic MEM' approach, which means maximizing the Shannon-Jaynes entropy

$$S = -\sum_{i=1}^{n} \alpha_i \ln \alpha_i \tag{7}$$

under the condition of $\chi^2 = M$, where *M* is the total number of data points (i.e. the number of trajectories that have been analyzed). The χ^2 statistic is calculated from

$$\chi^2 = \sum_{j=1}^{M} \frac{\left(F(D_{e,j}) - \mathrm{ecdf}(D_{e,j})\right)}{\sigma_j^2}, \tag{8}$$

where σ_j^2 is the variance on the j^{th} data point of the ecdf, which can be calculated from[9]:

$$\sigma_j^2 = \frac{j(M-j+1)}{(M+1)^2(M+2)}. \tag{9}$$

For the determination of σ_j^2 we note that the experimental error on $\overline{\xi}$ (and hence D_e) caused by the limited localization accuracy of the trajectory locations $\vec{r}_i$ can effectively be neglected. This is because the distance between subsequent points $\vec{r}_i$ is typically 10 pixels, while the localization

uncertainty is typically less than 30% of a pixel. This means that the variance σ_j^2 can be attributed to limited sampling statistics alone.

The MEM analysis was implemented in Matlab using the function 'fmincon' from the Optimization Toolbox. The constraint $\chi^2 = M$ was relaxed to the narrow interval $M - \sqrt{2M} \le \chi^2 \le M + \sqrt{2M}$, where χ^2 is calculated according to Eq. (8). Eq. (8), in turn, makes use of Eq. (9) and Eq. (6), the latter being calculated using the Matlab function 'gamcdf'. The function value $\mathrm{ecdf}\left(D_{e,j}\right)$ was simply calculated as $j/N+1$. In this work, the discretisation space D_i was chosen as a logarithmic scale of n points (user defined, typically n=50) starting at half the minimal D_e value from the experiment and ending at twice the maximum D_e value. Given the set of empiric diffusion coefficients D_e as determined by fSPT, the MEM routine then calculates the corresponding fractions α_i. Using the Stokes-Einstein relation from Eq. (3), this is finally converted to the corresponding size distribution.

SUPPLEMENTARY RESULTS

Simulations

From the trajectories determined by fSPT, the diffusion coefficient of individual particles can be calculated. However, as explained in the 'Theory' section of the Supporting Information, the precision with which the empirical diffusion coefficient is determined depends on the number of steps available in the trajectory. When a system of particles with a distribution of diffusion coefficients is measured by fSPT, the resulting distribution of empirical diffusion coefficients will be broadened by this statistical inaccuracy compared to the real distribution, as expressed by Eq. (4). We have, therefore, developed a maximum entropy method (MEM) that is capable of removing this statistical broadening to a large extent from the raw measurements. To evaluate and demonstrate the value of this approach, we have performed computer simulations where we have taken a heterogeneous population of particles with a distribution of diffusion coefficients that follows a double lognormal function. As can be seen from Figure S1a, the first lognormal component has a maximum at D = 0.94 $\mu m^2/s$ and the second component at D = 2.55 $\mu m^2/s$. From this double lognormal distribution, 2000 diffusion coefficients were selected using the Matlab function 'lognrnd', which corresponds to an fSPT experiment in which 2000 particles are tracked. For each diffusion coefficient, a random walk trajectory of 10 steps was simulated. Next, for each trajectory the empirical diffusion coefficient was calculated, the distribution of which is shown in Figure S1b. Due to the statistical broadening it is clear that the two lognormal components cannot be distinguished anymore. However, after applying the MEM analysis, the two lognormal components again can be clearly resolved and the obtained distribution is very close to the true underlying distribution.

Validation of fSPT against DLS

The fSPT sizing technique was first validated against standard DLS measurements using dispersions of fluorescent nanospheres with a nominal diameter of 0.1 µm and 0.2 µm and coated with PLA. We will conveniently refer to both types of particles as 100 nm and 200 nm beads, respectively. An example of an fSPT recording of 200 nm spheres diffusing in water is shown in the Supplementary Movie 1. An excellent agreement was found between the DLS and fSPT size measurements. The average diameter measured for the 100 nm nanospheres by DLS and fSPT was d_{DLS} = 121.8 nm and d_{SPT} = 121.1 nm, respectively. Similarly, for the 200 nm nanospheres we found d_{DLS} = 235.5 nm and d_{SPT} = 239.1 nm. While average sizes and the modes of the size distributions correspond very well for DLS and fSPT, it is clear that the DLS size distribution is much broader than the fSPT distribution (Fig. S2a and S2b). This is because fSPT has the advantage of having several measurements for each individual particle (i.e. the number of steps within each trajectory, 10 in this case), while DLS analysis depends on single fluctuations. The superior resolution of fSPT compared to DLS can also be seen from the data in Fig. 2c where a mixture of 100 and 200 nm nanospheres was measured by DLS and fSPT. Contrary to DLS, fSPT with MEM analysis can indeed resolve both populations. In this particular experiment there were less 100 nm than 200 nm spheres. To demonstrate more clearly the capability of the MEM analysis technique to separate two populations of particles that differ in size by only a factor of two, the trajectories from the 100 nm sample were pooled with an equal number of trajectories from the 200 nm sample. As is shown in Fig. 2d, the MEM technique indeed nicely resolves both components, with the two modes corresponding to the modes that have been found

for the individual populations. Furthermore, when comparing the raw size distributions with the ones after MEM analysis in Fig. S2, it is clear that MEM analysis also reduces small features that can be attributed to statistical sampling noise. MEM analysis therefore also avoids over-interpretation of features in the raw size distributions that are not statistically warranted by the data.

Let it be noted that the experimental conditions were chosen such as to represent the typical experimental situation throughout this study, i.e. particles of 100 nm and 200 nm in size and trajectory lengths of 10 steps. For these conditions it was demonstrated that the resolving power of fSPT with MEM analysis is at least a factor of two. This is, however, no fundamental limit, as the resolving power will increase for the same conditions if longer trajectories would be available (aslo refer to Eq. (2) in the Theory section). This in turn is limited by the camera sensitivity (illumination time per frame) and the camera speed (maximum number of frames per second). As camera technology will improve over the years, the resolving power of fSPT with MEM analysis is expected to increase correspondingly.

fSPT sizing of polystyrene nanoparticles in full human serum

Apart from measuring very accurate and precise size distributions, the real power of fSPT lies in its ability to measure size distributions of fluorescently labeled particles in biological fluids. Measuring particle sizes by DLS in fluids such as serum is very difficult or even impossible due to the many light scattering components. This is evident from the results in Figure S3 where 100 nm nanospheres were measured in freshly collected human serum by both DLS and fSPT. Even at the highest concentration of particles (1/10 dilution of stock) no meaningful results could be obtained by DLS since the particle signal is indistinguishable from the signal generated by the serum components (see Fig. S3a). By fSPT however, the particles (1/400 dilution of stock) were clearly visible and a reliable size distribution could be calculated. Compared to buffer the average size has increased by approximately 15 nm and the distribution is somewhat broadened, which is most likely because of serum proteins adhering to the beads (see Fig. S3b).

Influence of the fluorescence label

To verify that aggregation of liposomes in blood is not influenced by the particular choice of fluorescence label, a control experiment was performed using the same type of liposomes, but carrying a different fluorophore. To this end, 10% DSPE-PEG DOTAP-DOPE liposomes were labeled with with an equal amount of DiO (3,3' - Dioctadecyloxacarbocyanine iodide) instead of Rhodamine-B. The DOTAP-DOPE liposomes containing 10% of DSPE-PEG were chosen since they exhibit controlled aggregation (see Fig. 3a) which will allow for a direct comparison. The DiO labeled liposomes were mixed with whole blood (n=3) and their size was measured every 30 min over a 2 hour period. As is clear from the results in Fig. S4a, the aggregation over time is completely similar to the same type of liposomes labeled with Rhodamine-B (compare with Fig. 3a). This shows that the choice of fluorophore did not influcence the fSPT sizing experiments.

Another control experiment was performed on the cell-derived microparticles collected from human microvascular endothelial cells in culture. The microparticles were labeled with FITC and TRITC using

a primary antibody against uPA and a FITC and TRITC labeled secondary antibody. The FITC and TRITC labeled microparticles were spiked to human microparticle-free undiluted plasma and measured by fSPT (*n*=2). As is clear from the results in Fig. S4b, again we could not find any difference in size distribution due to the different labels. This is another confirmation that the results reported here were not influenced by the choice of fluorophore.

SUPPLEMENTARY FIGURES

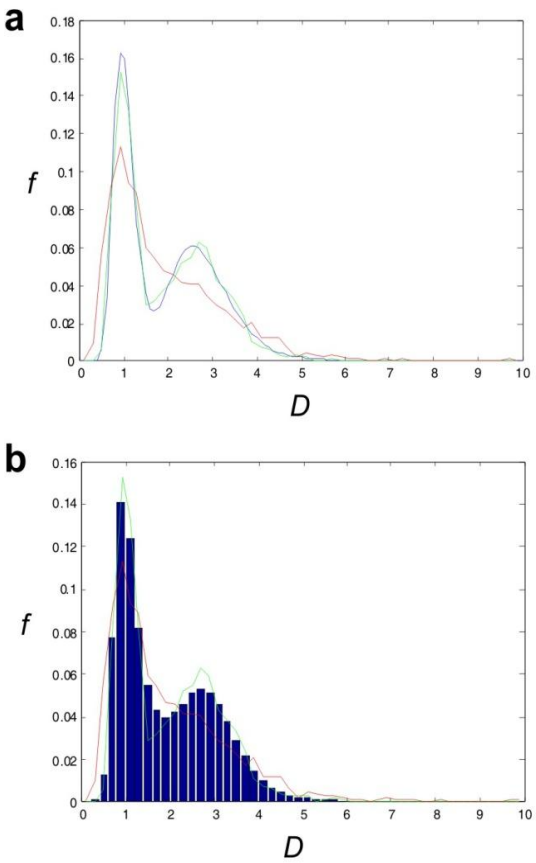

Figure S1: **Performance of fSPT MEM analysis.** (a) The blue line represents the distribution of diffusion coefficients of a heterogeneous population of particles according to a double lognormal distribution. From this distribution, 2000 diffusion coefficients have been selected at random, resulting in the distribution indicated in green. Trajectories of 10 steps have been simulated for each of the 2000 diffusion coefficients, from which a distribution of empirical diffusion coefficients D_e is obtained as indicated in red. Due to statistical broadening the two major components in the original distribution cannot be discerned anymore. (b) After applying the MEM analysis to the set of 2000 empirical diffusion coefficients, the original distribution is nicely retrieved (blue bars) in which the two major components again can be resolved.

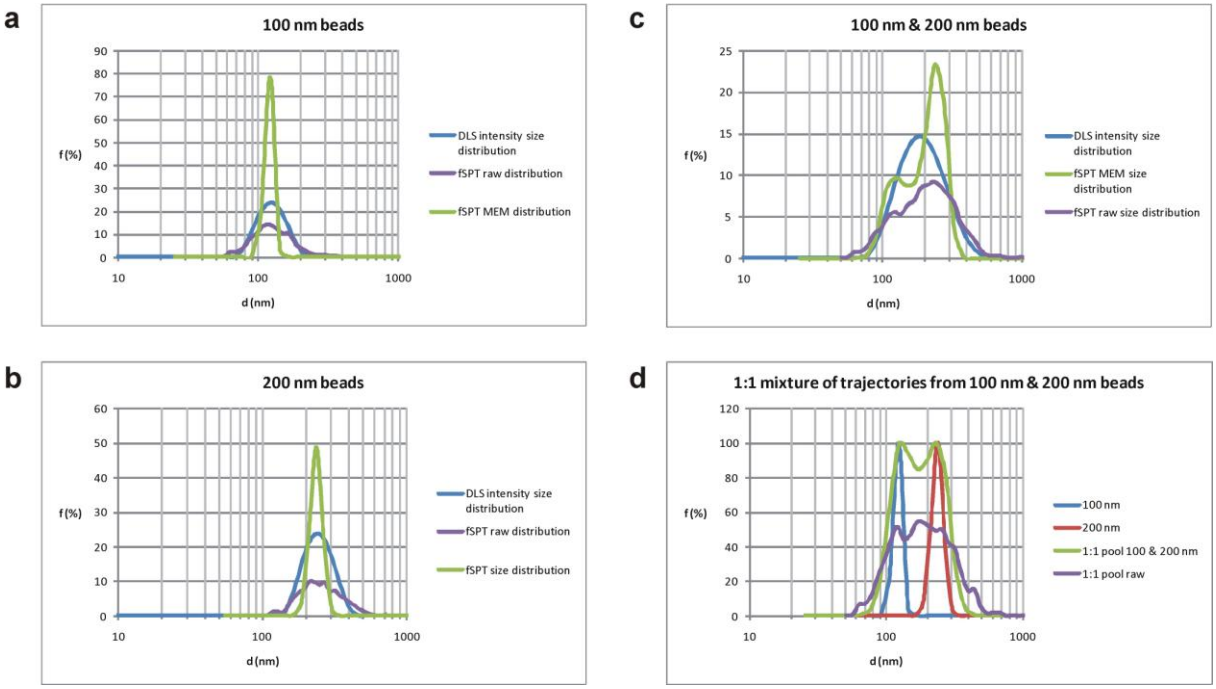

Figure S2: **Validation of fSPT size measurements.** (a) The size distributions obtained by DLS and fSPT for a suspension of fluorescent 100 nm spheres are shown. The fSPT size distribution is shown before and after MEM analysis, which demonstrates the gain in resolution obtained from MEM analysis. (b) The DLS and fluorescence SPT size distributions are displayed for 200 nm spheres before and after MEM analysis (c) A dispersion containing a mixture of 100 nm and 200 nm spheres was measured by DLS and fluorescence SPT. The two populations are clearly resolved after MEM analysis. (d) To demonstrate the capability of fluorescence SPT to separate two subpopulations that differ in size by a factor of 2 only, an equal number of 100 nm and 200 nm trajectories was pooled together and analyzed by the MEM technique. The size distributions of the individual populations (blue and red) as well as the result from the pooled data (green) are shown. For clarity, each distribution was normalized to its maximum value.

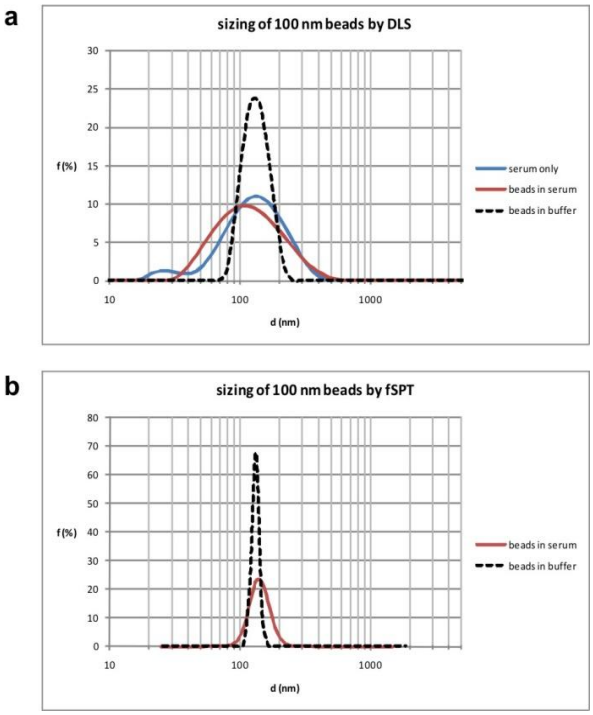

Figure S3: **Comparison of DLS and fSPT sizing in serum.** Size measurement of fluorescent 100 nm polystyrene beads in serum. (a) Using DLS, even at high particle concentrations the size distribution of the beads in serum (red) cannot be discerned from the signal arising from the serum itself (blue) due to its many light scattering components. (b) Using fSPT, however, the size of the beads can be accurately determined both in buffer and serum.

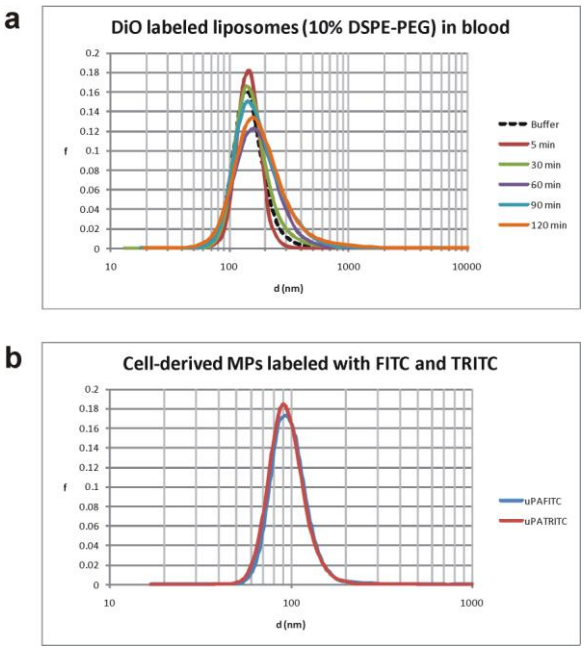

Figure S4: I**nfluence of the fluorescence dye on fSPT sizing in blood.** (a) 10% DSPE-PEG DOTAP-DOPE liposomes were labeled with DiO and dispersed in whole blood during 2 hours (*n*=3). The aggregation over time is analogous as was observed for the same type of lipomes labeled with Rhodamine-B (cfr. Fig. 3a). (b) uPA positive cell-derived microparticles were labeled with FITC and TRITC. After spiking in human plasma, the fSPT size distributions are entirely similar, demonstrating that the fluorphore did not influence the size measurements (*n*=2).

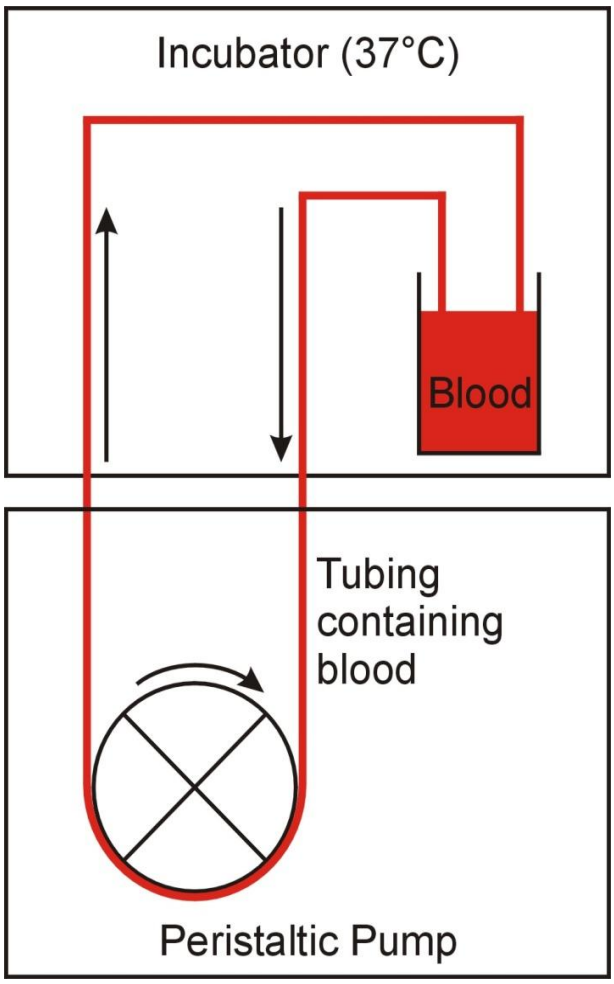

Figure S5: **Schematic illustration of artificial blood circulation system.** A basic artificial blood circulation system was constructed using a peristaltic pump, a small incubator chamber at 37°C containing a container with 5 ml of blood and tubing with 1.6 mm inner diameter. To study liposomal aggregation, the liposomes are injected into the tubing using a syringe. Small blood samples are taken at regular time intervals out of the blood container after injection and transferred to a microscope slide for fSPT size measurements.

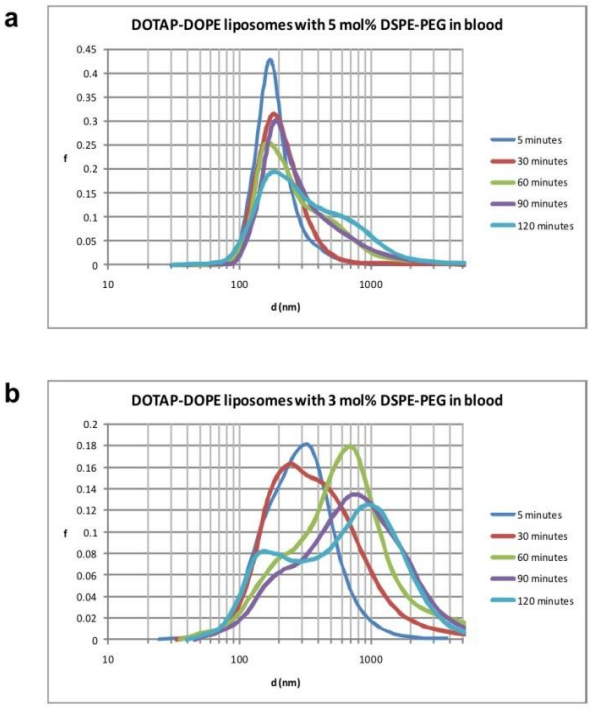

Figure S6: **Effect on aggregation in whole blood of the liposome pegylation degree.** Size distributions of DOTAP-DOPE liposomes with 5 mol% (a) and 3 mol% (b) DSPE-PEG are shown for various incubation times in blood as obtained by fSPT. The tendency to form aggregates increases as the degree of pegylation decreases.

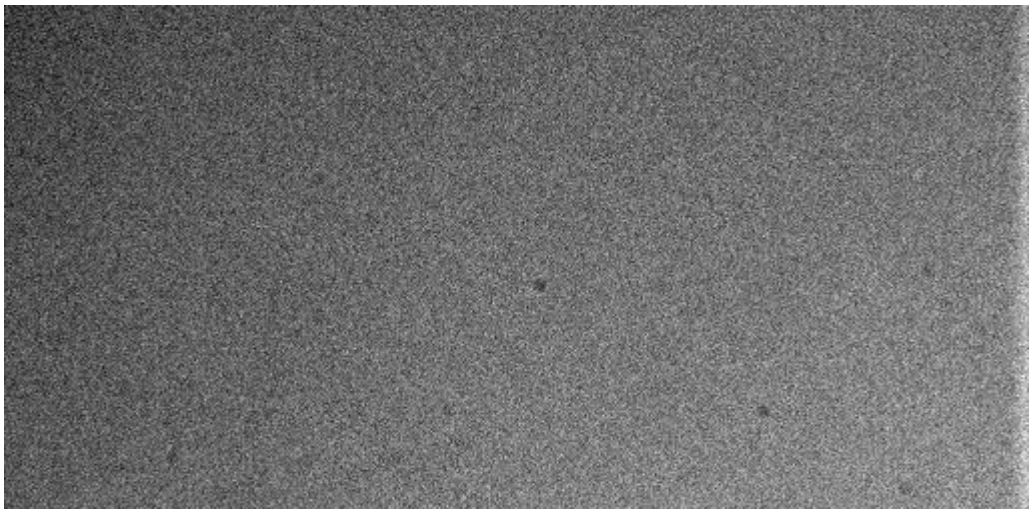

Figure S7: **Negative control for the detection of cell-derived microparticles in plasma.** Endothelial cell microparticles remain invisible after addition of the unrelated antibody against CD41 in human plasma (negative control).

SUPPLEMENTARY MOVIES

Supplementary Movie 1: Example fSPT movie of fluorescent 200 nm spheres diffusing in water. The motion trajectories are superimposed if the particle is detected for at least 10 consecutive steps. The frame rate was reduced twofold to 20 frames per second. The field of view is 23 µm by 23 µm.

Supplementary Movie 2: Example fSPT movie of fluorescently labeled DOTAP-DOPE liposomes in full human serum. The sample was collected from the artificial circulation system 120 min after addition of the liposomes. The playback rate is real-time at 40 frames per second. The field of view is 46 µm by 23 µm.

Supplementary Movie 3: Example fSPT movie of fluorescently labeled DOTAP-DOPE liposomes in human plasma. The sample was collected from the artificial circulation system 120 min after addition of the liposomes. The playback rate is real-time at 40 frames per second. The field of view is 46 µm by 23 µm.

Supplementary Movie 4a: Example fSPT movie of fluorescently labeled DOTAP-DOPE liposomes in whole blood. The sample was collected from the artificial circulation system 120 min after addition of the liposomes. The large aggregate has a diameter of almost 2 µm. Smaller particles are also present but cannot be seen for these contrast settings (see Supplementary movie 4b). The playback rate is real-time at 40 frames per second. The field of view is 46 µm by 23 µm.

Supplementary Movie 4b: The same movie as in Supplementary Movie 4a is shown with different contrast settings to demonstrate that also small liposomes are still present. The large aggregate is highly over-exposed and therefore seems much bigger.

Supplementary Movie 5: Endothelial microparticles can be detected in human plasma when labeled with Annexin V-FITC. The playback speed is real-time at 37 fps.

Supplementary Movie 6: Endothelial microparticles can be detected with a TRITC labeled antibody against CD105 in human plasma. The playback speed is real-time at 37 fps.

Supplementary Movie 7: Endothelial microparticles can be detected with a FITC labeled antibody against uPA in human plasma. The playback speed is real-time at 37 fps.

Bibliography

[1] L. Peeters, N. N. Sanders, K. Braeckmans, K. Boussery, J. V. de Voorde, S. C. De Smedt, J. Demeester, Vitreous: A barrier to nonviral ocular gene therapy, Investigative Ophthalmology & Visual Science, 46 (2005) 3553-3561.

[2] R. Lacroix, F. Sabatier, A. Mialhe, A. Basire, R. Pannell, H. Borghi, S. Robert, E. Lamy, L. Plawinski, L. Camoin-Jau, V. Gurewich, E. ngles-Cano, F. gnat-George, Activation of plasminogen into plasmin at the surface of endothelial microparticles: a mechanism that modulates angiogenic properties of endothelial progenitor cells in vitro, Blood, 110 (2007) 2432-2439.

[3] K. Braeckmans, K. Remaut, R. E. Vandenbroucke, B. Lucas, S. C. De Smedt, J. Demeester, Line FRAP with the confocal laser scanning microscope for diffusion measurements in small regions of 3-D samples, Biophysical Journal, 92 (2007) 2172-2183.

[4] J. C. Crocker and D. G. Grier, Methods of digital video microscopy for colloidal studies, Journal of Colloid and Interface Science, 179 (1996) 298-310.

[5] K. Braeckmans, D. Vercauteren, J. Demeester, and S. C. De Smedt, Single Particle Tracking, in:E. Diaspro (Ed.), Nanoscopy multidimensional optical fluorescence microscopy., Taylor and Francis, 2010.

[6] H. Qian, M. P. Sheetz, E. L. Elson, Single particle tracking. Analysis of diffusion and flow in two-dimensional systems, Biophys. J., 60 (1991) 910-921.

[7] A. K. Livesey and J. C. Brochon, Analyzing the Distribution of Decay Constants in Pulse-Fluorometry Using the Maximum-Entropy Method, Biophysical Journal, 52 (1987) 693-706.

[8] J. Skilling and R. K. Bryan, Maximum-Entropy Image-Reconstruction - General Algorithm, Monthly Notices of the Royal Astronomical Society, 211 (1984) 111-124.

[9] C. R. Mischke, A Distribution-Independent Plotting Rule for Ordered Failures, Journal of Mechanical Design-Transactions of the Asme, 104 (1982) 593-597.